

# Anomalous screening of quantum impurities by a neutral environment

E. Yakaboylu and M. Lemeshko

IST Austria (Institute of Science and Technology Austria), Am Campus 1, 3400 Klosterneuburg, Austria

(Dated: June 25, 2022)

It is a common knowledge that an effective interaction of a quantum impurity with an electromagnetic field can be screened by surrounding charge carriers, whether mobile or static. Here we demonstrate that very strong, ‘anomalous’ screening can take place in the presence of a neutral, weakly-polarizable environment, due to an exchange of orbital angular momentum between the impurity and the bath. Furthermore, we show that it is possible to generalize all phenomena related to isolated impurities in an external field to the case when a many-body environment is present, by casting the problem in terms of the angulon quasiparticle. As a result, the relevant observables such as the effective Rabi frequency, geometric phase, and impurity spatial alignment are straightforward to evaluate in terms of a single parameter: the angular-momentum-dependent screening factor.

It is quite intuitive that once an impurity is immersed in a dielectric medium, its response to an external electromagnetic field is reduced – or ‘screened’ – due to redistribution of charges in the dielectric [1]. This classical description implies that if the medium is neutral and only weakly-polarizable, it induces a negligible change in impurity-light interactions, if any at all. Physics becomes more complicated, however, when quantum effects come into play. There, even the vacuum can behave as a medium with a finite dielectric permittivity due to virtual pair fluctuations, with non-linear effects taking place in the presence of strong electric fields [2]. These quantum fluctuations can also screen the impurity charge in a medium. A typical example of the latter effect is the charged impurity screening in graphene [3]. Furthermore, due to the electron-phonon interactions, the Coulomb potential between two charged particles is screened in various settings, such as the jellium model [4]. Another important example is the Kondo screening, where the dipole moments of magnetic impurities are screened by conduction electrons [5, 6].

Here we uncover another type of screening – that due to exchange of orbital angular momentum between the impurity and the surrounding quantum many-body bath. While such a screening takes place even for a bath ‘blind’ to an electromagnetic field, it results in an anomalous decrease of the impurity susceptibility parameters, such as the effective dipole moment and polarizability. We start from the most general Hamiltonian describing an impurity interacting with a time-dependent electromagnetic (EM) field, which in the electric dipole approximation is given by:

$$\hat{H}_{\text{imp-em}}(t) = \hat{H}_{\text{imp}} - \hat{\mathbf{d}} \cdot \mathbf{E}(t). \quad (1)$$

Here  $H_{\text{imp}}$  is the Hamiltonian of the impurity,  $\hat{\mathbf{d}}$  is its corresponding electric dipole operator, and  $\mathbf{E}(t)$  is the electric field component of the EM field. The simplest Hamiltonian for an impurity possessing orbital angular momentum is given by  $H_{\text{imp}} = B\hat{\mathbf{L}}^2$ , where  $\hat{\mathbf{L}}$  is the angular momentum operator. The constant  $B$  depends on the particular system under investigation. For example, for the kinetic energy of a linear-rotor molecule,  $B = 1/(2I)$  is the rotational constant with  $I$  the moment of inertia [7] (we use the units of  $\hbar \equiv 1$  hereafter). For  $t_{2g}$ -electron orbitals in solids,  $B = -\mathcal{J}/2$ , where

$\mathcal{J}$  parametrizes Hund’s exchange coupling [8]. Further degrees of freedom, such as electronic and nuclear spins, electron hopping, or a crystal field, will result in additional terms in  $H_{\text{imp}}$ . For some other systems, such as highly-excited Rydberg electrons [9], or complex polyatomic molecules [10], the impurity Hamiltonian might assume an overall different form. However, since the effects discussed in this paper originate from the orbital angular momentum transfer, the qualitative picture is not expected to change substantially.

In the presence of a neutral many-particle environment, the full Hamiltonian of the system is given by:

$$H(t) = H_{\text{imp-em}}(t) + H_{\text{bath}} + H_{\text{imp-bath}}. \quad (2)$$

Note that we assume the environment to be weakly-polarizable, and therefore neglect its coupling to an external field. However, the impurity-bath interactions (of electrostatic, induction and dispersion type) are still present [11]. We consider a neutral bosonic bath as described by the Hamiltonian,  $H_{\text{bath}} = \sum_{k,\lambda\mu} \omega_k \hat{b}_{k\lambda\mu}^\dagger \hat{b}_{k\lambda\mu}$ , with  $\omega_k$  the dispersion relation. Here  $\hat{b}_{k\lambda\mu}^\dagger$  and  $\hat{b}_{k\lambda\mu}$  are the bosonic creation and annihilation operators,  $\sum_k \equiv \int dk$ , and  $k$ ,  $\lambda$ , and  $\mu$  label the corresponding quantum numbers of linear momentum, angular momentum and its projection on the  $z$ -axis, respectively [12–14]. Such a bath can be represented e.g. by lattice phonons [15], Bogoliubov excitations in a Bose-Einstein Condensate (BEC) [16], or phonons, rotons, and ripplons in superfluid helium [17]. For simplicity, in what follows we will refer to the bosonic excitations as ‘phonons.’ As it has been shown in Refs [12–14], the interaction of an impurity carrying orbital angular momentum with a bosonic bath can be described as:

$$H_{\text{imp-bath}} = \sum_{k,\lambda\mu} U_\lambda(k) \left[ Y_{\lambda\mu}^*(\hat{\theta}, \hat{\phi}) \hat{b}_{k\lambda\mu}^\dagger + Y_{\lambda\mu}(\hat{\theta}, \hat{\phi}) \hat{b}_{k\lambda\mu} \right], \quad (3)$$

where  $U_\lambda(k)$  is the angular-momentum-dependent coupling strength. As the interaction depends on the angle operators of the impurity via the spherical harmonics  $Y_{\lambda\mu}(\hat{\theta}, \hat{\phi})$ , the impurity in the angular state  $|jm\rangle$  can undergo a transition to  $|j'm'\rangle$  by absorption or emission of a phonon with the quantum numbers  $k, \lambda, \mu$ .

In principle, it is extremely challenging to obtain exact time-dependent solutions to the full Hamiltonian of Eq. (2). The

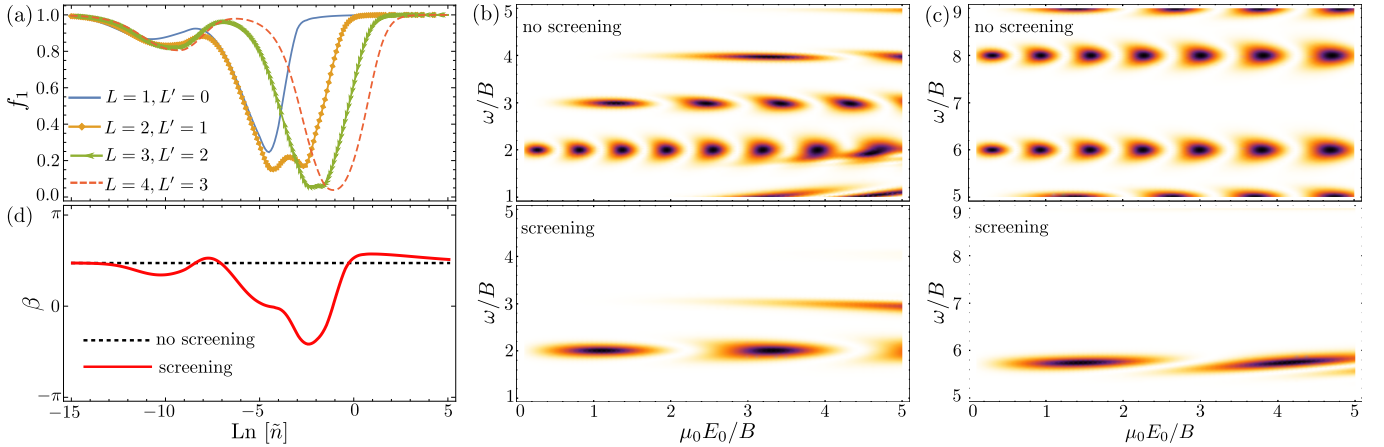


FIG. 1. (Color online) (a) Angular-momentum-dependent screening factor  $f_1^{L,L'}$ , for selected values of  $L, L'$ . (b) Total absorption of a free ground-state impurity (top), compared to a screened one, at bath density  $\text{Ln} [\tilde{n}] = -4.5$  (bottom); (c) Total absorption of a free impurity in the  $L = 3$  state (top), compared to a screened one, at bath density  $\text{Ln} [\tilde{n}] = -1.0$  (bottom); (d) Geometric phase of the screened impurity (solid line) compared to that of a free impurity (dashed line), as a function of bath density. See text.

problem can be simplified tremendously, however, if one approaches it from the perspective of quasiparticles. Namely, it has been recently shown that impurities whose orbital angular momentum is coupled to a many-body bath form the angulon quasiparticles [12–14, 18–20]. This novel kind of quasiparticles can be thought of as a non-Abelian counterpart of polarons [21], as it represents a quantum rotor dressed by a many-body bosonic field. Furthermore it was demonstrated that the predictions of the angulon theory are in good agreement with experiment for molecules in superfluid helium nanodroplets [22, 23].

Accordingly, the full Hamiltonian of Eq. (2) can be rewritten as  $H(t) = H_A - \hat{\mathbf{d}} \cdot \mathbf{E}(t) \otimes \mathbf{1}$ , where  $H_A = H_{\text{imp}} + H_{\text{bath}} + H_{\text{imp-bath}}$  is the angulon Hamiltonian, and the identity operator indicates that only the impurity interacts with the electric field. Taking only single-phonon excitations into account, the angulon eigenstate  $|A_{LM}\rangle$  can be approximated by the following variational ansatz [12]:

$$|A_{LM}\rangle = \sqrt{Z_L}|0\rangle|LM\rangle + \sum_{k\lambda\mu jm} \beta_{k\lambda j}^L C_{jm,\lambda\mu}^{LM} \hat{b}_{k\lambda\mu}^\dagger |0\rangle|jm\rangle, \quad (4)$$

with  $L$  and  $M$  being the total angular momentum and its projection on the laboratory-frame  $z$ -axis, respectively. Here  $|0\rangle$  represents the vacuum of bath excitations,  $C_{jm,\lambda\mu}^{LM} \equiv \langle LM|jm; \lambda\mu\rangle$  are the Clebsch-Gordan coefficients [24], and  $Z_L$  and  $\beta_{k\lambda j}^L$  are the variational parameters. Eq. (4) is straightforward to understand in the quasiparticle language: the first term corresponds to a bare impurity, with  $Z_L$  being the quasiparticle weight, while the second term describes the field of many-particle excitations due to the impurity-bath interactions.

We start with the first-order expansion of the electric dipole operator,  $\hat{\mathbf{d}} \cdot \mathbf{E}(t) \approx \hat{\mu}_0 \cdot \mathbf{E}(t)$  (higher-order terms will be discussed below). Here  $\hat{\mu}_0$  is the permanent dipole moment operator of the impurity [25]. In the angulon basis the state vector can be written as  $|\psi(t)\rangle = \sum_{LM} K_{LM}(t)|A_{LM}\rangle$ , where the evolution of the corresponding amplitudes,  $K_{LM}$ , is given by the

Schrödinger equation:

$$i \frac{dK_{LM}}{dt} = \varepsilon_L K_{LM} - \sqrt{\frac{4\pi}{3}} \sum_{L'M'q} K_{L'M'} E_q(t) |\mu_0| \langle A_{LM} | Y_{1q}(\hat{\theta}, \hat{\phi}) \otimes \mathbf{1} | A_{L'M'} \rangle, \quad (5)$$

where  $\varepsilon_L = \langle A_{LM} | H_A | A_{LM} \rangle$ , and we expressed  $\hat{\mu}_0 \cdot \mathbf{E}(t)$  in the spherical basis.

The matrix element in Eq. (5) is evaluated as:

$$\langle A_{L'M'} | Y_{1q}(\hat{\theta}, \hat{\phi}) \otimes \mathbf{1} | A_{LM} \rangle = \langle L'M' | Y_{1q}(\hat{\theta}, \hat{\phi}) | LM \rangle f_n^{L,L'} \quad (6)$$

where we separated out the factor,

$$f_n^{L,L'} = \sqrt{Z_{L'}^*} \sqrt{Z_L} + \begin{pmatrix} L' & n & L \\ 0 & 0 & 0 \end{pmatrix}^{-1} \sum_{k\lambda j j'} \beta_{k\lambda j}^{L'*} \beta_{k\lambda j}^L \times (-1)^{L+L'+\lambda+j'} \sqrt{2j'+1} C_{j' 0 n 0}^{j 0} \begin{Bmatrix} j & \lambda & L \\ L' & n & j' \end{Bmatrix}, \quad (7)$$

which we will refer to as the ‘angular-momentum-dependent screening factor.’ The round and curly brackets in Eq. (7) denote the Wigner  $3j$ -, and  $6j$ -symbols, respectively [24]. We see that the same selection rules that applied to the angular momentum of the bare impurity, now apply to the *total* angular momentum of the angulon,  $L$ . Therefore, we can rewrite Eq (5) as the Schrödinger equation for a single particle – the angulon – interacting with an EM field:

$$i \frac{dK_{LM}}{dt} = \varepsilon_L K_{LM} - \sqrt{\frac{4\pi}{3}} \sum_{L'M'q} K_{L'M'} E_q(t) f_1^{L,L'} |\mu_0| \langle LM | Y_{1q}(\hat{\theta}, \hat{\phi}) | L'M' \rangle. \quad (8)$$

The only difference is that now the effective dipole moment,  $f_1^{L,L'} |\mu_0|$ , which determines the coupling between the impurity

and the EM field, depends on the angular state of the impurity via the screening factor  $f_1^{L,L'}$ , in analogy to the energy-dependent susceptibility of QED vacuum [26]. Note that in the limit of  $\beta_{k,l,j}^L \rightarrow 0$ ,  $Z_L \rightarrow 1$ , and hence  $f_n^{L,L'} \rightarrow 1$ , Eq. (8) reduces to the usual Schrödinger equation of an isolated impurity interacting with the EM field. As we show below, the angular-momentum-dependent screening factor gives rise to the anomalous screening of the impurity, and the angulon theory provides a transparent physical explanation for this phenomenon.

In order to illustrate the effect of the bath on impurity-field interactions, we evaluate several observables, such as the effective Rabi frequency, geometric phase, and spatial alignment of the impurity axes. Without loss of generality, we consider a bath with the Bogoliubov dispersion relation,  $\omega_k = \sqrt{\epsilon_k(\epsilon_k + 2g_{bb}n)}$  [16], where  $\epsilon_k = k^2/(2m)$  with  $m$  the boson mass and  $n$  the boson particle density, and  $g_{bb} = 4\pi a_{bb}/m$  where we set the boson-boson scattering length to  $a_{bb} = 3.3/\sqrt{mB}$ . We choose the impurity-boson interaction as that derived for an ultracold molecule interacting with a dilute BEC,  $U_\lambda(k) = \sqrt{8nk^2\epsilon_k/(\omega_k(2\lambda + 1))} \int dr r^2 v_\lambda(r) j_\lambda(kr)$  where  $j_\lambda(kr)$  is the spherical Bessel function [12]. We model the angular-momentum-dependent coupling using Gaussian functions,  $v_\lambda(r) = u_\lambda(2\pi)^{3/2} e^{-r^2/(2r_\lambda^2)}$ , and focus on the leading  $\lambda$  orders, setting the parameters to  $u_0 = 1.75u_1 = 218B$ , and  $r_0 = r_1 = 1.5/\sqrt{mB}$ . Taking into account higher-order couplings with  $\lambda \geq 2$  will alter the selection rules on the boson-impurity scattering, however, is not expected to change the results qualitatively.

We study the behavior of the system as a function of the dimensionless bath density,  $\tilde{n} \equiv n(mB)^{-3/2}$ , and for the sake of simplicity, we consider a linearly polarized EM field  $\mathbf{E}(t) = E(t)\hat{z}$ , where  $E(t) = \mathcal{E}(t)\cos(\omega t)$  with the field frequency  $\omega$ , and the field envelope  $\mathcal{E}(t)$ . In the specified field direction we identify  $|\mu_0| \equiv \mu_0$  and  $Y_{1q}(\hat{\theta}, \hat{\phi})\sqrt{4\pi/3} = \cos(\hat{\theta})$ . Furthermore as the linearly polarized field preserves cylindrical symmetry, the magnetic quantum number will not change. In what follows, we focus on the  $M = 0$  manifold and omit the index  $M$ .

In Fig. 1(a) we present the angular-momentum-dependent screening factor for different angular-momentum states, as a function of the bath density. While for very low and very high densities the screening factor does not vary with  $\tilde{n}$  and  $L, L'$  substantially, a non-trivial dependence is observed for the intermediate densities. In particular, there occur pronounced minima in the screening factor for each angular-momentum state. The latter correspond to the instabilities accompanied by the transfer of angular momentum from the impurity to the many-body bath [12]. Such a drastic decrease in the screening factor due to the angular momentum transfer is the manifestation of the anomalous screening.

Let us now evaluate the total absorption of an impurity inside a neutral bath, as given by  $\mathcal{T}_L = 1 - |\langle A_L | U(t_f, t_i) | A_L \rangle|^2$ . Fig. 1(b) shows  $\mathcal{T}_L$  as a function of the applied field energy,  $\mu_0 E_0$ , and the EM frequency,  $\omega$ , without a bath and in the presence of it. The applied EM pulse is given by  $\mathcal{E}(t) = E_0 \exp[-4 \ln(2) t^2/\tau^2]$ , with the FWHM pulse duration  $\tau =$

$6\pi/B$  and the field amplitude  $E_0$ . Close to the resonance, the dynamics is dominated by Rabi oscillations, which correspond to peaks in absorption (dark shade in the figure). Thus, the peaks at  $\omega/B = 2, 3$ , and  $4$  correspond to the single-photon  $L = 0 \rightarrow L = 1$  transition, two-photon  $L = 0 \rightarrow L = 2$  transition, and three-photon  $L = 0 \rightarrow L = 3$  transition, respectively. From the bottom panel of Fig. 1(b), we observe that the neutral many-body environment leads to a drastic decrease of the effective Rabi frequency compared to the free impurity, which is a manifestation of the anomalous screening. Accordingly, we can identify the many-body induced Rabi frequency through the angular-momentum-dependent screening factor  $f$ :

$$\Omega_{L,L'}^A = f_1^{L,L'} \mu_0 E_0 \langle L | \cos(\hat{\theta}) | L' \rangle = f_1^{L,L'} \Omega_{L,L'} . \quad (9)$$

For instance, for the  $L = 0 \rightarrow L = 1$  transition the Rabi frequency is given by  $\Omega_{0,1}^A = \mu_0 E_0 f_1^{0,1} / \sqrt{3}$ . At the instability density of  $\ln[\tilde{n}] = -4.5$ , we obtain  $f_1^{0,1} \approx 1/4$ , which is consistent with the plots shown in Fig 1 (b). A similar behavior is observed for the total absorption for the impurity prepared in the third excited state,  $L = 3$ , see Fig. 1(c).

Another phenomenon which can be well explained in terms of the screening factor is the geometric phase accumulated during a cyclic evolution in the presence of a many-body environment. Geometric phase was first introduced by Berry within the context of adiabatic approximation [27]. Nevertheless, as pointed out by Aharonov and Anandan in their seminal paper [28], any cyclic evolution, whether adiabatic or non-adiabatic, may result in a geometric phase as given by  $\beta = \phi + \int_0^\tau dt \langle \psi(t) | H(t) | \psi(t) \rangle$ , where the second term refers to the dynamical phase. Let us start from one of the angulon eigenstates,  $|\psi_L(0)\rangle = |A_L\rangle$ , and let it evolve during a time interval  $\tau$  into the same state up to a phase,  $|\psi_L(\tau)\rangle = \exp(i\phi)|A_L\rangle$ . The following parameters  $\omega = 20B$ ,  $\mathcal{E}(t) = E_0 \sin^2(\pi t/\tau)$ ,  $\tau = 30/B$ , and  $E_0 = 11B$  bring the system back to the initial state after the time  $\tau$  for all densities. In Fig. 1 (d), we show the resulting geometric phase for the  $L = 1$  angulon state as a function of bath density.

In order to get more insight into how a neutral many-body environment influences the geometric phase, let us consider a two-level angulon system in a constant electric field, which is a good approximation for resonant driving as the dynamics occurs within two levels, such as  $L = 0$  and  $L = 1$ . The corresponding Hamiltonian can be written as  $\mathcal{H} = \sigma_0 R_0 + \boldsymbol{\sigma} \cdot \mathbf{R}$ , with some  $R_0$  and  $\mathbf{R}$ , where  $\sigma_0$  and  $\boldsymbol{\sigma}$  are the identity matrix and the vector of Pauli matrices, respectively. The time-evolution operator is given by:

$$U(t, 0) = \exp(-iR_0 t) \left( \sigma_0 \cos(Rt) - \frac{\mathbf{R}}{R} \cdot \boldsymbol{\sigma} \sin(Rt) \right) \quad (10)$$

with  $R \equiv |\mathbf{R}|$ . The state evolution is cyclic under the period of  $\tau = \pi/R$  up to the total phase  $\phi = \pi(1 - R_0/R)$ . The dynamical phase, on the other hand, is given by  $-\int_0^T dt \langle \psi_L(t) | H(t) | \psi_L(t) \rangle = -\pi(R_0 \pm R_z)/R$ , which leads to

$$\beta = \pi(1 \pm \cos(\gamma)) , \quad (11)$$

with  $\cos(\gamma) = R_z/R$ . For example, for the ground state, the geometric phase

$$\beta = \pi \left( 1 + \frac{\varepsilon_0 - \varepsilon_1}{\sqrt{(\varepsilon_0 - \varepsilon_1)^2 + (2f_1^{0,1} \mu_0 E_0 / \sqrt{3})^2}} \right). \quad (12)$$

As for the Rabi frequency, the neutral many-body environment affects the geometric phase through the screening factor  $f$ . As a result, depending on the bath density, the geometric phase changes, as shown in Fig. 1(d). Furthermore,  $\beta$  can assume both smaller and larger values compared to the isolated impurity case, and vanishes identically for certain densities.

As a final example we consider effects of a neutral bath on the time-evolution of the impurity spatial alignment due to a far-off-resonant laser pulse. Such a setting was realized e.g. in recent experiments on adiabatic [29] and non-adiabatic [23, 30, 31] molecular alignment in superfluid helium nanodroplets. Since in the case of intense off-resonant laser fields the second-order effects are important, we expand the dipole-field interaction as  $\hat{\mathbf{d}} \cdot \mathbf{E}(t) \approx \mu_0 E(t) \cos(\hat{\theta}) + (\Delta\alpha \cos^2(\hat{\theta}) + \alpha_{\perp}) E^2(t)/2$ , where  $\Delta\alpha = \alpha_{\parallel} - \alpha_{\perp}$  with  $\alpha_{\parallel}$  and  $\alpha_{\perp}$  being the polarizabilities in the direction parallel and perpendicular to the molecular axis. Furthermore, far from any resonances, the electric field can be averaged over the laser period so that the Hamiltonian is written in terms of the field envelope [32–34]:

$$H(t) = H_A - \frac{\Delta\alpha \mathcal{E}^2(t)}{4} \tilde{Y}_{2,0}(\hat{\theta}) \otimes \mathbf{1}, \quad (13)$$

where  $\tilde{Y}_{2,0}(\hat{\theta}) \equiv \sqrt{16\pi/45} Y_{2,0}(\hat{\theta})$ , and the constant energy shifts are omitted. Similar to the permanent dipole case, Eq. (6) turns the many-body Hamiltonian (13) into a corresponding single particle Hamiltonian with the replacement  $\Delta\alpha \rightarrow f_2^{L,L'} \Delta\alpha$ . The density dependence of the screening factor  $f_2$  is shown in Fig. 2(a).

Since an intense laser field aligns the molecule along the direction of maximum polarizability, which is the molecular axis for linear molecules [35, 36], it is convenient to quantify the degree of alignment using the alignment cosine,  $\langle \cos^2(\hat{\theta}) \rangle \equiv \langle \psi(t) | \cos^2(\hat{\theta}) | \psi(t) \rangle$ . If the pulse duration,  $\tau$ , is long compared to the rotational period,  $T_{\text{rot}} = 1/(2Bc)$ , the alignment process is adiabatic. In such a case, the alignment cosine follows the electric field envelope. As an example, we consider a  $\text{CS}_2$  molecule, whose parameters are given by:  $\Delta\alpha = 67.5 \text{ a.u.}$ ,  $\alpha_{\perp} = 35.76 \text{ a.u.}$ ,  $B = 0.109 \text{ cm}^{-1} = 4.97 \cdot 10^{-7} \text{ a.u.}$  In Fig. 2(b) we compare the time evolution of  $\langle \cos^2(\hat{\theta}) \rangle$  for an adiabatic alignment of a  $\text{CS}_2$  molecule inside a many-body environment of various densities to that of an isolated  $\text{CS}_2$ . We used the following parameters of the EM field:  $\omega = 800 \text{ nm}$ ,  $\tau = 300 \text{ ps}$ , the envelope  $\mathcal{E}(t) = E_0 \exp[-4 \ln(2) t^2 / \tau^2]$ , and intensity  $I = 2.4 \times 10^{10} \text{ W/cm}^2$  ( $I \equiv E_0^2 3.5 \times 10^{16} \text{ W/cm}^2$  in atomic units of  $E_0$ ). One can see that the screening manifests itself through a substantial reduction of the peak alignment. The magnitude of the screening depends on the  $f_2$ -factor and is straightforward to illustrate by considering a two-level system, consisting of  $L = 0$  and  $L = 2$ . For adiabatic alignment the state vector can be

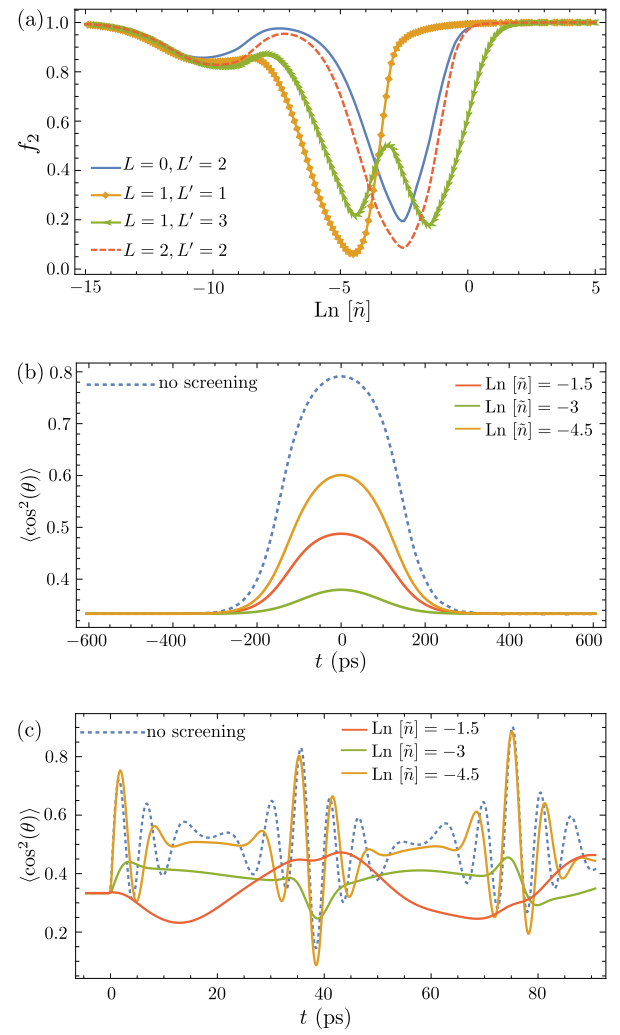


FIG. 2. (Color online) (a) The angular-momentum-dependent screening factor  $f_2^{L,L'}$ , for selected values of  $L, L'$ . (b) Adiabatic alignment of a free  $\text{CS}_2$  molecule in a bath of selected densities, as illustrated by the time evolution of the alignment cosine; (c) Same as (b), for the case of non-adiabatic alignment. See text.

defined as the instantaneous eigenstate of the Hamiltonian (13), furthermore the peak value of the alignment corresponds to the peak of the EM field envelope. For example, for the ground angulon state

$$\langle \cos^2(\hat{\theta}) \rangle_{\text{max}} = \frac{1}{3} + \left( \frac{2 - 2 \cos(\gamma)}{21} + \frac{2}{3\sqrt{5}} \sin(\gamma) \right), \quad (14)$$

where

$$\cos(\gamma) = \frac{\varepsilon_2 - \varepsilon_0 - f_2^{2,2} \Delta\alpha E_0^2 / 21}{\sqrt{(\varepsilon_2 - \varepsilon_0 - f_2^{2,2} \Delta\alpha E_0^2 / 21)^2 + (f_2^{0,2} \Delta\alpha E_0^2 / (3\sqrt{5}))^2}}. \quad (15)$$

As the screening factor  $f_2^{0,2}$  decreases, the peak alignment decreases as well. From Fig. 2(a) one can see that the screening factor  $f_2^{0,2}$  is drastically reduced for the density of  $\ln[\tilde{n}] = -2.5$ , which explains the substantial reduction of the peak

alignment shown in Fig. 2(b).

On the other hand, if the pulse period  $\tau$  is much smaller than the rotational period, the impurity-field interaction is non-adiabatic, which results in the revivals in the alignment cosine [37, 38]. Fig. 2(c) shows the time dependence of  $\langle \cos^2(\hat{\theta}) \rangle$  following a short pulse with  $\tau = 450$  fs and  $I = 2.4 \times 10^{12}$  W/cm<sup>2</sup> for a CS<sub>2</sub> molecule. As the rotational period depends only on the rotational constant  $B$ , the frequency of the revivals in the presence of a bath is similar to that of an isolated molecule. The maximum alignment depends on the screening factor  $f_2$ , as in the case of adiabatic molecule-field interactions.

Thus, we have shown that a neutral weakly-polarizable environment can induce a drastic screening of the impurity-field interactions due to the angular momentum transfer between the impurity and the bath. We developed a transparent analytic model based on the angulon quasiparticle, where all of the effects due to the bath are encapsulated in a single parameter – the angular-momentum-dependent screening factor  $f$ . Such a quasiparticle-based approach allows to extend the techniques developed for isolated atoms, molecules, and solid-state defects in external fields to the case when a many-particle environment is present. The predicted effects should be measurable with the state-of-the-art techniques used in quantum impurity experiments. For instance, the geometric phase can be measured using the impurity interference techniques [39–42], while experiments on molecules rotating in superfluid helium nanodroplets allow to perform spectroscopic and alignment measurements [23, 29–31, 43, 44]. The presented formalism can also be generalized to the case of a fermionic environment, such as an ultracold degenerate Fermi gas [45] or <sup>3</sup>He [16, 46], as well as to Bose-Fermi mixtures [47], which would further extend its domain of applicability.

We are grateful to G. Bighin, S. Meuren, and B. Midya for valuable discussions. E. Y. acknowledges financial support received from the People Programme (Marie Curie Actions) of the European Union's Seventh Framework Programme (FP7/2007-2013) under REA grant agreement No. [291734]

- [10] P. F. Bernath, *Spectra of atoms and molecules*, 2nd ed. (Oxford University Press, 2005).
- [11] A. Stone, *The Theory of Intermolecular Forces* (Oxford University Press, 2013).
- [12] R. Schmidt and M. Lemeshko, Phys. Rev. Lett. **114**, 203001 (2015).
- [13] M. Lemeshko and R. Schmidt, *Molecular impurities interacting with a many-particle environment: from ultracold gases to helium nanodroplets*, book chapter in "Low Energy and Low Temperature Molecular Scattering" edited by A. Osterwalder and O. Dulieu (Royal Society of Chemistry, 2016).
- [14] R. Schmidt and M. Lemeshko, Phys. Rev. X **6**, 011012 (2016).
- [15] G. D. Mahan, *Many-particle physics*, Physics of solids and liquids (Plenum, New York, NY, 1990).
- [16] L. P. Pitaevskii and S. Stringari, *Bose-Einstein Condensation and Superfluidity* (Oxford University Press, 2016).
- [17] F. Stienkemeier and K. K. Lehmann, J. Phys. B **39**, R127 (2006).
- [18] B. Midya, M. Tomza, R. Schmidt, and M. Lemeshko, Phys. Rev. A **94**, 041601(R) (2016).
- [19] E. S. Redchenko and M. Lemeshko, Chem. Phys. Chem. **117**, 3649 (2016).
- [20] X. Li, R. Seiringer, and M. Lemeshko, arXiv: 1610.04908 (2016).
- [21] J. T. Devreese, arXiv:1012.4576 (2015).
- [22] M. Lemeshko, arXiv preprint arXiv:1610.01604 (2016).
- [23] B. Shepperson, A. A. Sndergaard, L. Christiansen, J. Kaczmarczyk, M. Lemeshko, R. E. Zillich, and H. Stapelfeldt, in preparation (2016).
- [24] D. A. Varshalovich, A. Moskalev, and V. Khersonskii, *Quantum theory of angular momentum* (World Scientific, 1988).
- [25] P. W. Atkins and R. S. Friedman, *Molecular quantum mechanics* (Oxford university press, 2011).
- [26] M. Peskin and D. Schroeder, (1995).
- [27] M. V. Berry, Proceedings of the Royal Society of London. A. Mathematical and Physical Sciences **392**, 45 (1984).
- [28] Y. Aharonov and J. Anandan, Phys. Rev. Lett. **58**, 1593 (1987).
- [29] D. Pentlehner, J. H. Nielsen, L. Christiansen, A. Slenczka, and H. Stapelfeldt, Physical Review A **87**, 063401 (2013).
- [30] D. Pentlehner, J. H. Nielsen, A. Slenczka, K. Mølmer, and H. Stapelfeldt, Phys. Rev. Lett. **110**, 093002 (2013).
- [31] L. Christiansen, J. H. Nielsen, D. Tobias, V. Pentlehner, J. G. Underwood, and H. Stapelfeldt, Phys. Rev. A **92**, 1050 (2015).
- [32] B. Friedrich and D. R. Herschbach, Nature **353**, 412 (1991).
- [33] B. Friedrich and D. Herschbach, The Journal of Physical Chemistry **99**, 15686 (1995).
- [34] B. Friedrich and D. Herschbach, Phys. Rev. Lett. **74**, 4623 (1995).
- [35] H. Stapelfeldt and T. Seideman, Rev. Mod. Phys. **75**, 543 (2003).
- [36] R. Torres, R. de Nalda, and J. P. Marangos, Phys. Rev. A **72**, 023420 (2005).
- [37] J. Ortigoso, M. Rodrígues, M. Gupta, and B. Friedrich, Journal of Chemical Physics **110**, 3870 (1999).
- [38] M. Lemeshko, R. V. Krems, J. M. Doyle, and S. Kais, Molecular Physics **111**, 1648 (2013).
- [39] J. E. Hoffman, K. McElroy, D.-H. Lee, K. M. Lang, H. Eisaki, S. Uchida, and J. C. Davis, Science (2002), 10.1126/science.1072640.
- [40] T. Hanaguri, Y. Kohsaka, J. Davis, C. Lupien, I. Yamada, M. Azuma, M. Takano, K. Ohishi, M. Ono, and H. Takagi, Nature Physics **3**, 865 (2007).
- [41] G. M. Rutter, J. Crain, N. Guisinger, T. Li, P. First, and J. Stroscio, Science **317**, 219 (2007).
- [42] S. Jeon, B. B. Zhou, A. Gyenis, B. E. Feldman, I. Kimchi, A. C. Potter, Q. D. Gibson, R. J. Cava, A. Vishwanath, and A. Yazdani,

---

- [1] J. D. Jackson, *Classical Electrodynamics* (John Wiley and Sons, 1962).
- [2] A. Di Piazza, C. Müller, K. Z. Hatsagortsyan, and C. H. Keitel, Rev. Mod. Phys. **84**, 1177 (2012).
- [3] I. S. Terekhov, A. I. Milstein, V. N. Kotov, and O. P. Sushkov, Phys. Rev. Lett. **100**, 076803 (2008).
- [4] M. Brack, Rev. Mod. Phys. **65**, 677 (1993).
- [5] J. Kondo, Progress of theoretical physics **32**, 37 (1964).
- [6] M. Medvedyeva, A. Hoffmann, and S. Kehrein, Phys. Rev. B **88**, 094306 (2013).
- [7] H. Lefebvre-Brion and R. W. Field, *The Spectra and Dynamics of Diatomic Molecules* (Elsevier, New York, 2004).
- [8] A. Georges, L. de' Medici, and J. Mravlje, Annu. Rev. Condens. Matter Phys. **4**, 137 (2013).
- [9] T. F. Gallagher, *Rydberg atoms* (Cambridge University Press, 2005).

Nature materials **13**, 851 (2014).

[43] R. Lehnig, P. L. Raston, and W. Jäger, Faraday Discuss. **142**, 297 (2009).

[44] J. P. Toennies and A. F. Vilesov, Angewandte Chemie International Edition **43**, 2622 (2004).

[45] B. DeMarco and D. S. Jin, Science **285**, 1703 (1999).

[46] A. J. Leggett, *Quantum Liquids: Bose Condensation and Cooper Pairing in Condensed-Matter Systems* (Oxford, 2006).

[47] K. Günter, T. Stöferle, H. Moritz, M. Köhl, and T. Esslinger, Phys. Rev. Lett. **96**, 180402 (2006).